Catalysis Today 168 (2011) 147–157

Contents lists available at ScienceDirect

Catalysis Today

journal homepage: www.elsevier.com/locate/cattod

A comparative study of diffusion of benzene/p-xylene mixtures in MFI particles, pellets and grown membranes

R. Kolvenbach[a], N. Al-Yassir[b], S.S. Al-Khattaf[b], O.C. Gobin[a], J.H. Ahn[a], A. Jentys[a,*], J.A. Lercher[a]

[a] Department of Chemistry, Technische Universität München, Lichtenbergstraße 4, 85747 Garching, Germany
[b] Center of Research Excellence in Petroleum Refining and Petrochemicals, King Fahd University of Petroleum & Minerals, Dhahran, 31261, Saudi Arabia

ARTICLE INFO

Article history:
Received 1 December 2010
Received in revised form 14 January 2011
Accepted 17 January 2011
Available online 25 February 2011

Keywords:
ZSM-5
Silicalite-1 membranes
Aromatic molecules
Knudsen diffusion
Stefan–Maxwell diffusion
Wicke–Kallenbach experiments
Pressure modulation frequency response

ABSTRACT

The transport and separation of mixtures between benzene and p-xylene in pellets prepared by pressing of ZSM-5 powder and a dense supported (crystalline) Silicalite-1 membrane were compared to isolated ZSM-5 crystallites. The kinetics of the transport in the pressed pellet and the grown membrane determined in a Wicke–Kallenbach cell (313–403 K; partial pressure range 200–2300 Pa) differed significantly from those measured for isolated ZSM-5 particles with the pressure modulation frequency response technique (343–403 K; partial pressure 30 Pa). In a pressed pellet, the transport was of Knudsen type leading to high fluxes of 10^{-4} mol/m^2 s and identical permeances for benzene and p-xylene. The diffusion coefficient in a pressed pellet exceeded that in particles, in which the transport was controlled by intracrystalline diffusion and the pore entrance step, by 8 orders of magnitude. The flux across a grown Silicalite-1 membrane was two orders of magnitude lower and the permeability of p-xylene was 2.6–5 times higher than that of benzene. The change in diffusivity in the membrane compared to the particles results from the higher surface coverage of p-xylene.

1. Introduction

The energy and cost efficient separation of hydrocarbons such as xylene isomers is a challenging task on the academic as well as on the industrial scale. The similar vapor pressure of the three xylene isomers makes the separation by distillation economically unfeasible. Therefore, the separation is performed on an industrial scale by preferential adsorption (Parex Process, UOP) or by fractional crystallization [1]. Both approaches require high energy input and high investments in the process equipment.

The continuous separation of p-xylene from a mixture of xylenes and other (substituted) aromatic molecules based on membranes [2–4,6,7,10–12] as well as on hierarchical zeolites [5] is one of the promising alternative approaches, which has been addressed in a large number of studies during the last years. These studies have led, however, to controversial results. Keizer et al. suggested that the separation of a binary mixture of p-xylene/o-xylene (at partial pressures of 0.31/0.26 kPa) is possible using a MFI membrane of 3 μm thickness utilizing the different minimum kinetic diameters of the molecules [6]. The flux of p-xylene in a mixture with o-xylene increased, whereas the o-xylene permeability decreased markedly compared to the transport of single components. The temperature dependency of the p-xylene permeance in mixtures resulted in an increase of the separation factor from below 2 to 25 in the temperature range from 293 to 473 K. This effect was attributed to size exclusion effects and the varying coverage of the external surface.

A much better separation was obtained by Sakai et al. employing MFI membranes with a thickness between 60 and 130 μm [7]. They reported a maximum in the separation factor for p-xylene of 250 at 473 K, applying a ternary xylene mixture with partial pressures of 0.3, 0.27 and 0.27 kPa for p-, o- and m-xylene, respectively. In agreement with Keizer et al. [6], this maximum was attributed to competitive diffusion and the adsorption effects. Interestingly, it was reported that the membrane permeability increased linearly with increasing p-xylene concentration, but was independent of the temperature.

A new approach for the separation of ternary xylene mixtures was presented by Daramola et al. [8,9] who used nanocomposite MFI-alumina hollow fiber membranes prepared via a pore plugging hydrothermal synthesis. A separation factor of 107 for p- and o-xylene was reported at 573 K for a mixture of p-, m- and o-xylene with partial pressures of 0.62 kPa/0.27 kPa/0.32 kPa, respectively. A maximum p-xylene flux of 4.5 μmol/(m^2 s) was reached. Most promising of this material is the increase of the surface to volume ratio by one order of magnitude compared to conventional membrane tubes, which allows building more compact and, therefore, more cost effective units.

In contrast, Falconer and Noble [10–12] reported a separation factor for o-xylene and p-xylene in a binary mixture for ZSM-5 and Silicalite-1 membranes of close to one over a temperature

* Corresponding author. Tel.: +49 089 289 13538; fax: +49 089 289 13544.
E-mail address: andreas.jentys@ch.tum.de (A. Jentys).

0920-5861/$ – see front matter © 2011 Elsevier B.V. All rights reserved.
doi:10.1016/j.cattod.2011.01.037

Nomenclature

A	surface area of one side of the pellet or membrane [m^2]
D	diffusion coefficient [m^2/s]
$E_{A,D}$	activation energy of diffusion [kJ/mol]
F	flow [mol/m^2s]
ΔH_{Ads}	heat of adsorption [kJ/mol]
L	characteristic length of diffusion [m]
M	molar mass of the molecules [g/mol]
N_{UC}	number of unit cells in the pellet [mol]
R	molar gas constant [J/(mol K)]
SO_{max}	maximum surface occupations [molecules/UC]
T	temperature [K]
c_A	concentration in the particle [mol/m^3]
c_F	concentration of the diffusing substance in the feed [mol/m^3]
c_0	concentration at the beginning of the experiment [mol/m^3]
c_∞	concentration inside the pellet at the end of the measurement [mol/m^3]
q_{sat}	saturation value of the surface occupation [mol/g]
r_p	average radius of the mesopores [m]
t	time [s]
$t_{transm.}$	the transmission time [s]
ρ	density of the adsorbent [g/m^3]
θ	normalized surface coverage [–]
$(1-\theta_i)_{ln}$	logarithmic mean of free vacancies [–]

range between 380 and 480 K. Notably, the permeances in the mixtures were lower than those for the single components, which was attributed to a single file transport mechanism (i.e., the faster permeating substance is retarded to the rates of the slower permeating molecule, as the molecules cannot pass each other inside the pores).

These latter data also indicate that the permeability of a molecule in a binary mixture through a zeolite-membrane may not be directly related to the diffusion coefficient in powder samples. Gobin et al. [13] reported recently intracrystalline diffusion coefficients of 5.28×10^{-13} and 2.46×10^{-13} m^2/s for benzene and p-xylene in ZSM-5 at 373 K, while the permeation fluxes of the same molecules through the Silicalite-1 membranes showed the opposite trend (10^8 and 3×10^8 mol/(s m^2 Pa) for benzene and p-xylene, respectively) [10].

Our aim in this work is to contribute to the understanding of the transport mechanism in MFI membranes and to address these discrepancies. The extension to pressed MFI pellets aims to describe the impact of compacting powder samples, which can serve as model for understanding the elementary transport processes in hierarchically structured zeolites, on the overall transport properties.

2. Experimental

2.1. Materials

H-ZSM-5 powder with a Si/Al ratio of 45 was provided by Süd-Chemie. SEM images (Fig. 1A) show that the sample consists of agglomerates with an average size of 360 ± 170 nm as determined by dynamic light scattering. The transmission electron micrograph, shown in Fig. 1B, illustrates a primary particle size of 50–100 nm, which agrees well with the estimate from the half-width of the reflexes in the X-ray diffraction pattern. The N_2 sorption isotherm indicates a BET surface area of 423 m^2/g and a micro-, meso-, and macropore volume of 0.12, 0.04 and 0.22 cm^3/g, respectively. The external surface area was 65 m^2/g. A detailed analysis of the material properties including the analysis of the transport mechanisms of aromatics can be found in Ref. [13].

The Silicalite-1 membranes were produced by the Fraunhofer Institute for Ceramic Technologies and Systems IKTS, with an average thickness of 30–60 μm. The Silicalite-1 samples are supported on an asymmetric pellet made of titanium-dioxide with a minimum pore size of 30 nm.

The adsorbates benzene and p-xylene (GC standard, >99.96%, Sigma–Aldrich) were used without further purification.

2.2. Physicochemical characterization

The N_2 physisorption isotherm and the SEM images were measured and analyzed according to Gobin et al. [13]. X-ray diffraction (XRD) patterns were recorded on a Rigaku Miniflix II XRD powder diffraction system using Cu Kα radiation ($\lambda_{K\alpha 1}$ = 1.54051 Å, 30 kV and 15 mA). The XRD patterns were recorded in the scanning mode from 5° to 60° (2θ) at a detector angular speed of 2°/min and step size of 0.02°.

The concentration and strength of acid sites were determined from IR spectra of adsorbed pyridine described in detail in Ref. [14].

2.3. Diffusion measurements by the Wicke–Kallenbach method

2.3.1. Experimental setup and sample preparation

The powdered ZSM-5 samples (100 mg) were pressed into a stainless steel ring and mounted into the Wicke–Kallenbach cell. Before the experiments the cell was flushed with He for 30 min followed by an activation of the samples at 823 K for 1 h using a heating rate of 10 K/min and a He flow of 50 ml/min. The grown membranes were placed between two stainless steel rings sealed with graphite. The activation procedure was performed identical to that with the pressed samples. On both sides of the sample a gas stream was flowing along the external surface of the pellet/membrane. One of the gas streams was loaded with the benzene, p-xylene or with a binary mixture, the other gas stream was the pure sweep gas. To avoid a pressure gradient over the pellet the flow rates of both gas streams were identical.

The flow rates were controlled by four mass flow controllers (Bronkhorst EL-flow select) and the temperature of the cell was controlled by an electronic PID controller (Eurotherm 2404). The loading of the gas stream with benzene and p-xylene was performed via two saturators, cooled to 15 °C in a thermostat to avoid the condensation of the hydrocarbons inside the system.

The concentration of the aromatic molecules in the permeate stream was followed at a time resolution of 22.5 s with a mass-spectrometer (WR 13302, Hiden Analytical).

2.3.2. Calculation of the diffusion coefficient

The diffusion through porous media under steady state conditions can be described by the first Fickian law [17]:

$$F = -D\frac{\delta c_A}{\delta_Z} \quad (1)$$

in which F is the flux [mol/(s m^2)], D the diffusion coefficient [m^2/s], c_A the concentration of the diffusing substance [mol/m^3] and z the coordinate in the direction of diffusion [m]. By assuming constant diffusivity the concentration profile over the membrane can be linearized as shown in Eq. (2).

$$\dot{n}_A = -D\frac{A}{L}(c_{A,L} - c_{A,O}) \quad (2)$$

with $\dot{n}_A$ being the transfer rate [mol/s], A the cross sectional area of the pellet [m^2], L the thickness of the pellet [m], $c_{A,L}$ the concentration on the permeate side and $c_{A,0}$ the inlet concentration

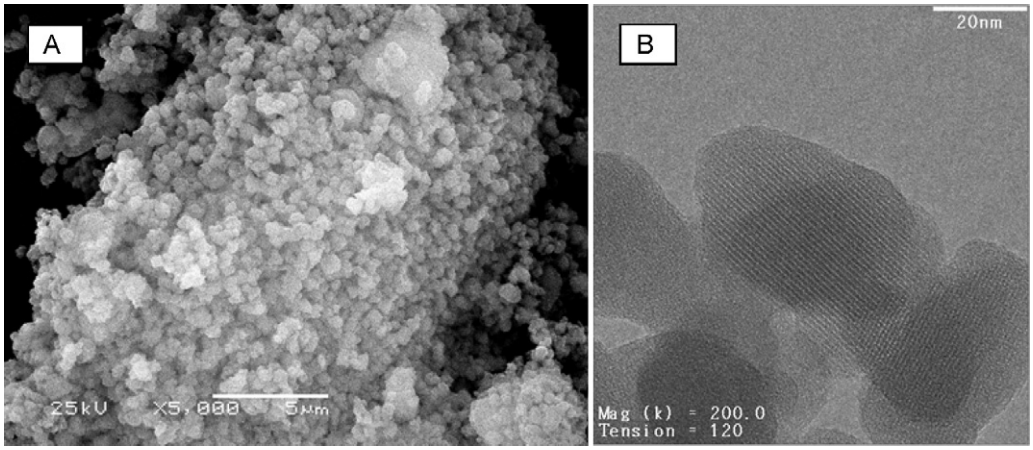

Fig. 1. SEM (left, A) and TEM (right, B) image of the ZSM-5 powder.

[mol/m^3]. The diffusion coefficient can be calculated from:(3)$D = \frac{L}{A} F_S \frac{x_{A,p}}{1-x_{A,p}}$ with F_S denoting the flow rate of the sweep gas [m^3/s] and $x_{A,p}$ the molar fraction of substance A in the permeate stream [–].

2.4. Pressure modulation frequency response experiments

2.4.1. Theoretical

In a typical experiment the volume is perturbed by a square wave with an amplitude in the order of ±1%, while the pressure is continuously monitored. Prior to the measurement the sorbate is equilibrated over the sample at a pressure in the linear part of the isotherm (Henry region). The pressure response can be mathematically described according to Yasuda [15] by two characteristic functions given by Eqs. (4) and (5), which are an in-of-phase and out-of-phase function of the mass balance of a closed volume.

$$\frac{p_B}{p} * \cos(\varphi - \varphi_B) - 1 = \sum_1^n K_n \delta_n^{in} \tag{4}$$

$$\frac{p_B}{p} * \sin(\varphi - \varphi_B) - 1 = \sum_1^n K_n \delta_n^{out} \tag{5}$$

$$K = \frac{R * T}{V_{FR}} * \left(\frac{d\theta}{dp}\right) \tag{6}$$

where p is the pressure amplitude of the experiment [Pa], p_B is the corresponding pressure amplitude in a blank experiment [Pa], φ is the phase difference between the perturbation and the response function [–], φ_B is the phase difference in a blank experiment [–]. δ_n^{in} and δ_n^{out} are the characteristic functions [–], n is the number of independent parallel transport processes occurring simultaneously [–]. K is proportional the slope of the adsorption isotherm, the temperature T [K], the volume of the system V_{FR} [m^3] and the gas constant R [J/(mol K)].

To account for the non-idealities arising from the apparatus itself, a blank experiment was carried out.

2.4.2. Experimental setup

The setup is an all metal high vacuum unit ($p_{base} < 10^{-6}$ Pa) equipped with volume modulation part, which consists of a magnetically driven plate sealed with two UHV bellows. The pressure is recorded online via a pressure transducer (Baratron MKS 16A11TCC). The adsorbing substrate is added via a separately pumped dosing line with an all metal regulating valve.

2.4.3. Sample preparation

30 mg of powdered sample was dispersed in a quartz sample holder on several layers of quartz wool to avoid bed effects. The glass-tube was connected to the vacuum setup, placed into an oven and pumped to 10^{-6} Pa. The samples were activated at 723 K for 1 h with a temperature ramp of 10 K/min in vacuum ($p < 10^{-4}$ Pa) to remove adsorbed water.

The adsorbate was added with a partial pressure of 30 Pa until the adsorption equilibrium was fully established. During the experiment the volume of the setup was changed periodically with a square wave volume perturbation function in a frequency range of 5 to 10^{-3} Hz and an amplitude of ±1% of the total system volume.

2.4.4. Data treatment

The amplitude and the phase lag were obtained from a Fourier transformation of the pressure response. The parameters of the characteristic functions (Eqs. (4)–(6)) were obtained by nonlinear parameter fitting using a CMA evolutional strategy in Matlab [16]. The optimization of the fitting was performed as described previously [13]. The solutions of the Fickian law for different limiting steps can be found in Refs. [13,15].

2.4.5. Gravimetric sorption and uptake rate measurements

Uptake rates of slowly diffusing adsorbates were determined in a microbalance (Seteram TGA-111). The samples (~10 mg) were dispersed on quartz wool in order to avoid bed effects and activated at 823 K for 1 h with an incremental heating rate of 10 K/min under vacuum ($p < 10^{-5}$ Pa). The uptake rates were obtained by following small pressure steps between 10 and 100 Pa at 373 K. Uptake curves were analyzed according to the 1D diffusion model developed by Crank [17].

3. Results

3.1. Physical state of the membranes

The pressed ZSM-5 pellet represents essentially an assembly of small particles with a size of 360 ± 170 nm and mesopores in between the particles. The pore size and volume of the pellet were determined from a nitrogen sorption isotherm (see Fig. 2 for comparison with the powdered material). The pressure region from the adsorption branch up to $p/p_0 = 0.25$ was nearly identical for the powder and the pellet indicating that the micropore volume remained unmodified by the compacting procedure. BET analysis [18] of the N_2 adsorption isotherm of the pellet resulted in a specific surface area of 446 m^2/g, which is identical to that of the isolated particles (420 m^2/g). The hysteresis in the sorption isotherm was

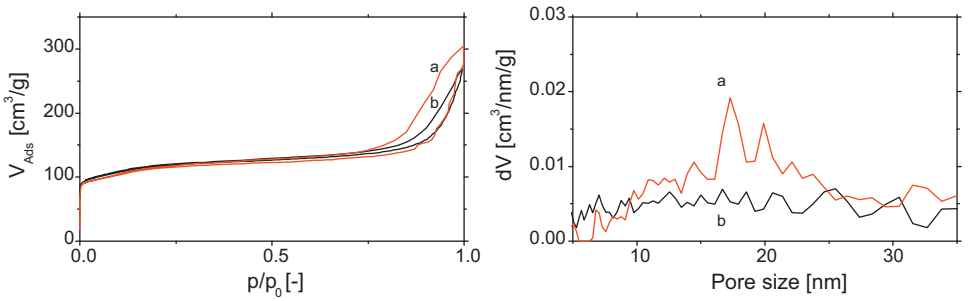

Fig. 2. Nitrogen sorption isotherm (left) and the corresponding pore size determined by DFT analysis (right) of the parent ZSM-5 material before (b) and after (a) pressing it to a pellet for Wicke–Kallenbach experiments.

observed at significantly lower p/p_0 values, i.e., 0.25 and 0.75 for the pressed powder and for the isolated particles, respectively, and the total area of the hysteresis loop obtained was much larger in the case of the pellet.

The total volume of the micro- and mesopores of the ZSM-5 powder and pellet was determined by using *t*-plot analysis according to the method of Halsey [19]. The results are summarized in Table 1. A total micropore volume of 0.147 cm^3/g was observed for both samples, while the mesopore volume increased from 0.132 cm^3/g to 0.232 cm^3/g in the pellet. The analysis of the pore size distribution of the pellet applying DFT analysis showed a maximum at 17 nm, whereas the minimum mesopore diameter was 6 nm (Fig. 2b).

The SEM images of the pellet and the membrane are shown in Fig. 3. On the surface of the pellet macropores exist between the isolated particles. In contrast, the grown membrane showed a texture composed of well-defined intergrown crystals of 50 μm diameter.

The XRD patterns of the Silicalite-1 membrane and of ZSM-5 were identical (Fig. 4A). Reflections assigned to the TiO_2 carrier of the membrane were present in Fig. 4B. The results of the acid site determination are summarized in Table 2.

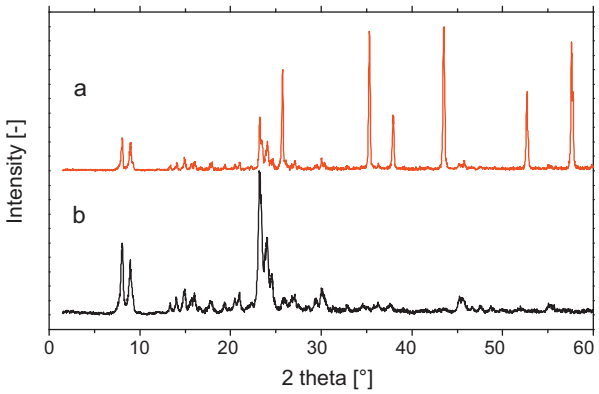

Fig. 4. XRD patterns of ZSM-5 zeolite (a) and Silicalite-1 membrane (b).

Table 1
Porosity of ZSM-5 in the powdered and the pressed form.

Material	SBET [m^2/g]	V_{Micro} [cm^3/g]	V_{Meso} [cm^3/g]
Parent	420	0.147	0.132
Pellet	446	0.147	0.232

3.2. Transport measurements

3.2.1. Zeolite particles

The diffusivities of benzene and p-xylene were determined by the frequency response method at 343 K, 373 K and 403 K. The results from a previous publication by Gobin et al. [13] are compiled in Table 3. The resulting characteristic functions were analyzed under the assumption that intracrystalline diffusion control determines the apparent diffusivity and that a Gaussian type particle size distribution exists (confirmed by DLS measurements [11,21]).

The out-of-phase functions of benzene and p-xylene at 403 K are compared in Fig. 5. The shape of both curves was similar without any broadening of the p-xylene response, which indicates that the diffusion process in small ZSM-5 particles is isotropic. Note that the transport of p-xylene in larger ZSM-5 particles (3 μm particle size) was found to be non-isotropic with a faster diffusion in the straight channel system [10,17,19].

The apparent diffusion coefficients of benzene and p-xylene in the small particles are two orders of magnitude smaller com-

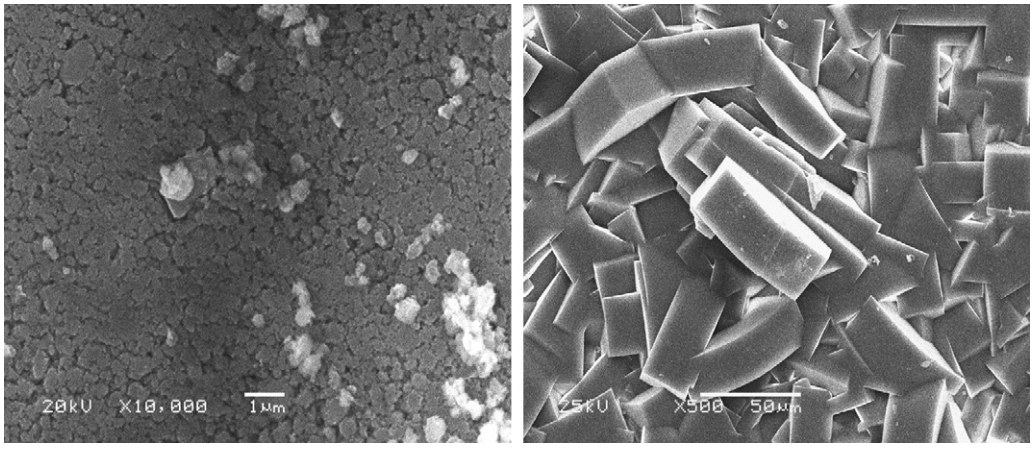

Fig. 3. SEM images of a pellet used for Wicke–Kallenbach experiments (left) and a grown Silicalite-1 membrane (right).

Table 2
Acid site concentration of ZSM-5 and Silicalite-1 membrane determined by IR spectroscopy of adsorbed pyridine.

Material	Brønsted acid sites [mmol/g]	Lewis acid sites [mmol/g]	Total acidity [mmol/g]
H-ZSM-5	0.360	0.091	0.451
Silicalite-1 membrane	0.0	0.011	0.011

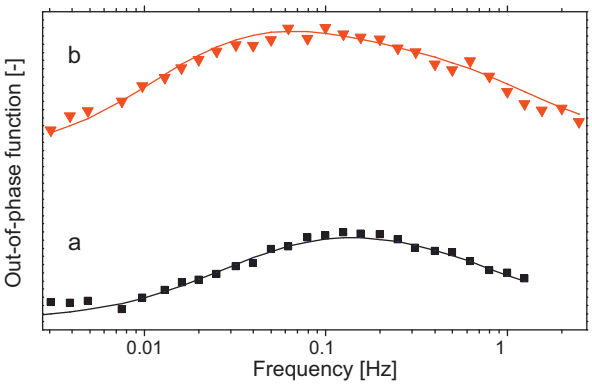

Fig. 5. Out-of-phase frequency response of benzene (a) and p-xylene (b) at 403 K. The fits (lines) were obtained by using a single diffusion model including a Gaussian particle size distribution and considering a surface resistance. The p-xylene curve is shifted by 0.2 [13].

pared to those in the large particles, whereas the time constants for diffusion (L^2/D) remain in the same order of magnitude. This has been attributed to the fact that the surface adsorption and the pore entrance step are controlling the rate of the overall transport due to the short length of the diffusion path in the small particles [13]. This conclusion has been supported by the apparent activation energies (Fig. 6 and Table 3). The obtained apparent activation energies in the small particles studied here are slightly higher than the ones observed in larger particles [13].

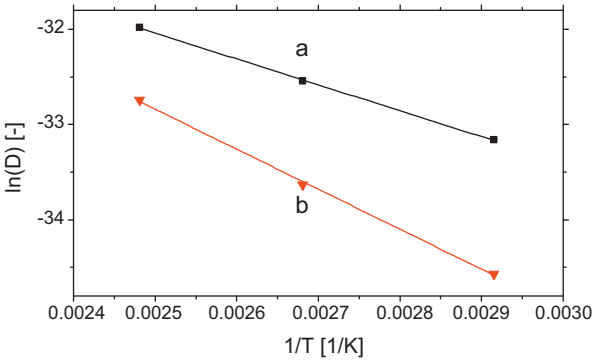

Fig. 6. Arrhenius plots for benzene (a) and p-xylene (b) of apparent diffusion on ZSM-5 powder [13].

3.2.2. Pressed pellets

Fig. 7 shows the transient fluxes of benzene and p-xylene mixtures in a pressed pellet (100 mg) at 343 K, 373 K and 403 K. The overall trends of the concentration traces were identical for all experiments. After an initial time period, a sharp increase of the flux was observed, followed by steady-state flux of both substances through the pellet. All experiments indicated an earlier breakthrough of benzene as the temperature increases. The benzene concentration at the eluate side exceeded the steady state concentrations shortly after the first appearance of benzene on the effluent side ("overshooting"). The steady state fluxes do not change between 343, 373 and 403 K (see Table 4) indicating that the permeabilities were identical for benzene and p-xylene and, therefore, a separation between these species is not possible.

The influence of the pellet weight (proportional to its thickness) on the transient flux examined using pellets of 150 mg, 100 mg and 50 mg weight (corresponding to 1.5, 1 and 0.5 mm thickness) is shown in Fig. 8. Two major trends can be observed. The fluxes decreased by 50%, when the pellet thickness is tripled and the "overshooting effect" of benzene was reduced with decreasing

Table 3
Transport data and fitting parameters obtained for a theoretical model assuming one apparent diffusion process Dapp with a Gaussian particle distribution as additional fitting parameter [13].

	T [°C]	L^2/D [s]	$D_{app} \times 10^{15}$ [m^2/s]	K	NRMS-Error	EA [kJ/mol]
Benzene	343	32.5	3.96	0.73	0.26	
$L = 3.59 \times 10^{-07}$ m	373	17.6	7.34	0.46	0.19	23
$\sigma = 2.12 \times 10^{-07}$ m	403	10.0	12.9	0.29	0.16	
p-Xylene	343	132.9	0.97	0.77	0.30	
$L = 3.59 \times 10^{-07}$ m	373	52.0	2.48	0.57	0.32	35
$\sigma = 2.32 \times 10^{-07}$ m	403	21.4	6.02	0.39	0.19	

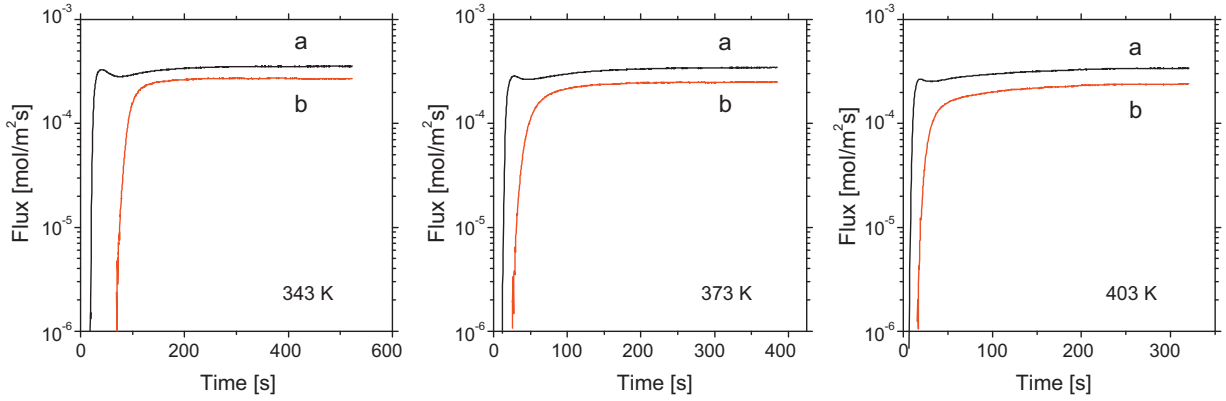

Fig. 7. Flux of benzene (a)/p-xylene (b) mixtures (313 Pa/234 Pa) in the Wicke–Kallenbach experiment on ZSM-5 at 343 K (left), 373 K (middle) and 403 K (right).

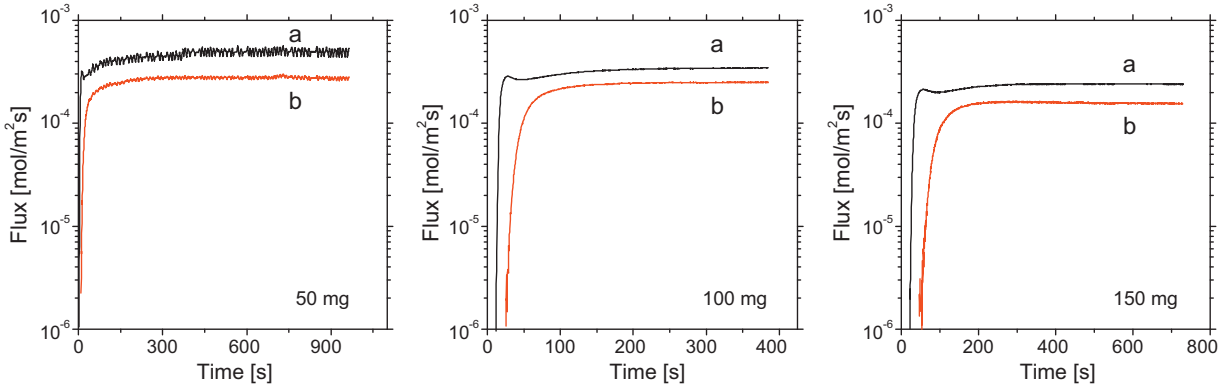

Fig. 8. Flux of benzene (a)/p-xylene (b) mixtures (313 Pa/234 Pa) in the Wicke–Kallenbach experiment on ZSM-5 as function of the pellet thickness at 373 K.

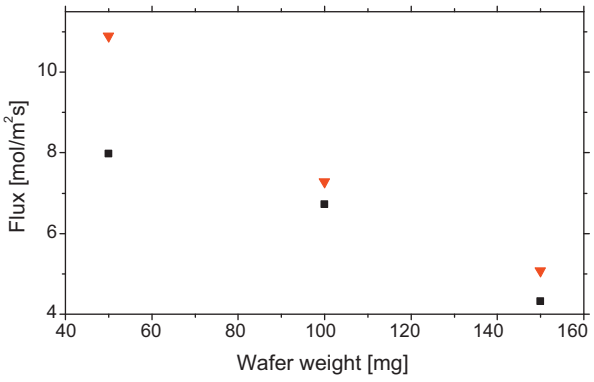

Fig. 9. Permeance as function of the pellet thickness for benzene (■)/p-xylene (▼) (313 Pa/234 Pa) on ZSM-5 at 373 K.

thickness and fully eliminated on the thinnest pellet. The ratio of the steady state permeances of benzene and p-xylene were not affected by the pellet thickness (see Fig. 9), while the overall fluxes decreased with the thickness. The time until breakthrough increased with increasing thickness. The obtained results with pressed pellets are summarized in Tables 4 and 5.

The gravimetric uptake rates of benzene and p-xylene were determined in a separate experiment (see Fig. 10). For benzene a diffusional time constant (L^2/D) of 1830 s was observed for a pressure step from 10 to 100 Pa corresponding to a diffusion coefficient of 1.36×10^{-10} m^2/s (assuming an infinite plain sheet model assumption [17] and a length of diffusion equal to the half of the wafer thickness). For p-xylene the time constant of diffusion was 57670 s resulting in a diffusion coefficient of 4.33×10^{-12} m^2/s. Note the model applied assumes a one dimensional diffusion process, which is a valid simplification for the case of the adsorption into a pellet.

3.2.3. Grown membranes

The experimental results with the grown Silicalite-1 membranes differ significantly. The molar flux was two orders of magnitude lower than that observed with the pressed pellet. Although the overall shape of the curves was similar to the pressed pellets, the temperature dependence was much stronger. As shown in Fig. 11, the "overshooting" effect of benzene decreased with increasing temperature turning into an exponential increase at 403 K. The p-xylene transient curves were exponential functions over the entire temperature range.

As with the pressed pellets, the time required for the concentration front to pass through the pellet was shortened with increasing temperature. However, the time required to establish equilibrium was much longer in comparison to the pressed pellets. Note that the lengths of the transmission times were identical for benzene and p-xylene at 343 K and 403 K, while at 313 K benzene passed faster through the membrane.

The fluxes and permeabilites of benzene, p-xylene and mixtures of both components are compiled in Tables 6 and 7, respectively.

Interestingly, the steady state concentrations indicate a higher permeability for p-xylene than for benzene in experiments with single components as well as with binary mixtures. The p-xylene permeation increased stronger with the temperature compared to that of benzene, therefore, the separation factor is higher than one and increases markedly with the temperature. The highest

Table 4
Steady state flux (F), breakthrough time ($t_{transm.}$) and the permeance (P) of benzene and p-xylene as well as the separation factor (S) for a pressed ZSM-5 pellet at 343 K, 373 K and 403 K.

T [K]	$F_{Benzene} \times 10^4$ [mol/(s m^2)]	$F_{p\text{-}Xylene} \times 10^4$ [mol/(s m^2)]	$t_{transm.,benzene}$ [min]	$t_{transm.,p\text{-}xylene}$ [min]	$P_{Benzene} \times 10^7$ [mol/(s m^2 Pa)]	$P_{p\text{-}Xylene} \times 10^7$ [mol/(s m^2 Pa)]	S
343	3.55	2.67	19	47	7.48	7.44	1.00
373	3.45	2.51	12	27	7.28	6.72	0.93
403	3.4	2.41	7	17	7.18	6.42	0.89

Table 5
Steady state flux (F), breakthrough time ($t_{transm.}$) and the permeance (P) of benzene and p-xylene as well as the separation factor (S) for a pressed ZSM-5 pellet with a weights of 50, 100 and 150 mg at 373 K.

W	$F_{Benzene} \times 10^4$ [mol/(s m^2)]	$F_{Benzene} \times 10^4$ [mol/(s m^2)]	$t_{transm.,benzene}$ [min]	$t_{transm.,p\text{-}xylene}$ [min]	$P_{Benzene} \times 10^7$ [mol/(s m^2 Pa)]	$P_{p\text{-}Xylene} \times 10^7$ [mol/(s m^2 Pa)]	S
50	5	2.75	3	9	10.9	7.98	0.73
100	3.45	2.51	12	27	7.28	6.72	0.93
150	2.39	1.55	23	47	5.08	4.31	0.85

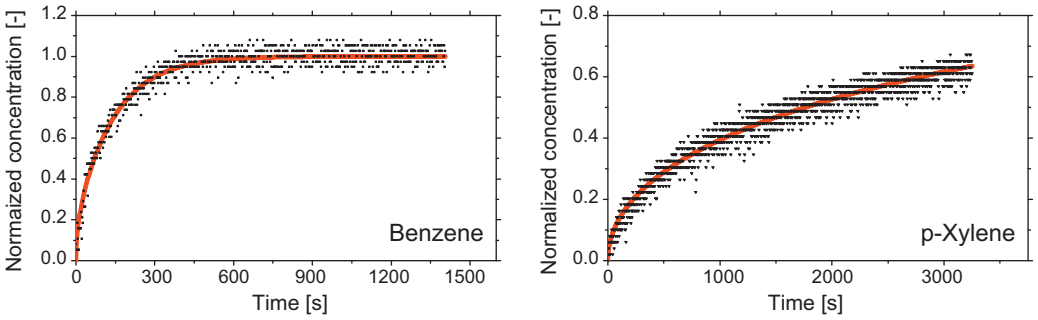

Fig. 10. Gravimetric uptake rates of benzene (left) and p-xylene (right) with the pressed ZSM-5 at 373 K, applying a pressure step from 10 to 100 Pa.

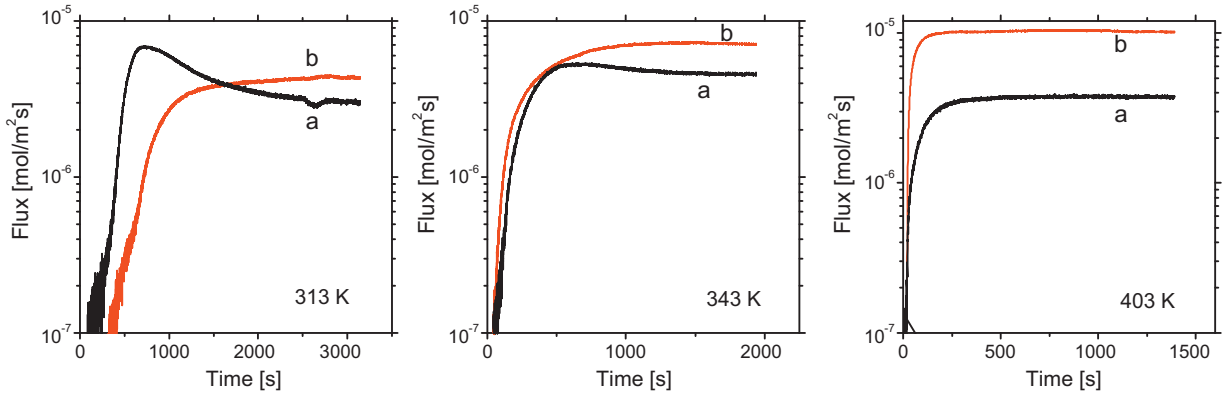

Fig. 11. Flux of benzene (a)/p-xylene (b) mixtures (578.7 Pa/322.9 Pa) in the Wicke–Kallenbach experiment on the Silicalite-1 membranes at 313 K, 343 K and 403 K.

Table 6
Single component fluxes (F) and permeances (P) of benzene (578.7 Pa) and p-xylene (322.9 Pa) obtained by Wicke–Kallenbach experiments using a Silicalite-1 membrane of 30–60 μm at 313 K, 343 K and 403 K.

T [K]	$F_{Benzene} \times 10^6$ [mol/(s m^2)]	$F_{p\text{-}Xylene} \times 10^6$ [mol/(s m^2)]	$P_{Benzene} \times 10^9$ [mol/(s m^2 Pa)]	$P_{p\text{-}Xylene} \times 10^9$ [mol/(s m^2 Pa)]
313	3.5	3.91	6.05	12.1
343	2.85	8.65	4.92	26.8
403	2.52	12.82	4.35	39.7

Table 7
Steady state flux (F), breakthrough time ($t_{transm.}$) and the permeance (P) of benzene and p-xylene as well as the separation factor (S) for a Silicalite-1 membrane at 343 K, 373 K and 403 K.

T [K]	$F_{Benzene} \times 10^6$ [mol/(s m^2)]	$F_{p\text{-}Xylene} \times 10^6$ [mol/(s m^2)]	$t_{transm.,benzene}$ [min]	$t_{transm.,p\text{-}xylene}$ [min]	$P_{Benzene} \times 10^9$ [mol/(s m^2 Pa)]	$P_{p\text{-}Xylene} \times 10^9$ [mol/(s m^2 Pa)]	S
313	2.98	4.34	350	500	5.2	13.55	2.63
343	4.56	7.24	60	60	7.9	22	2.78
403	3.72	10.13	17	18	6.5	31.5	4.76

ratio between the single component permeabilities of p-xylene and benzene (i.e., 8.6 shown in Table 6) was obtained at 403 K. This value decreased to 5 for the mixture of both components (578.7 Pa/322.9 Pa). The trend of the permeances of the single components compared to the binary mixtures as function of the temperature is shown in Fig. 12. The single component permeability for both adsorbates at 313 K was identical to the mixture, while it clearly differed at higher temperatures. Notably, the single component flux of p-xylene increased more rapidly than that in a mixture, which led to a decrease of the p-xylene permeance by 21% in a mixture with benzene at 403 K. In contrast, the permeability of benzene increased by 49% at 403 K compared to the diffusivity as a single component.

The fluxes of the single components in the examined crystalline Silicalite-1 membrane agreed well with those reported in Ref. [10]. Note however, that in contrast to the previous report, a separation of the benzene/p-xylene mixture can be achieved.

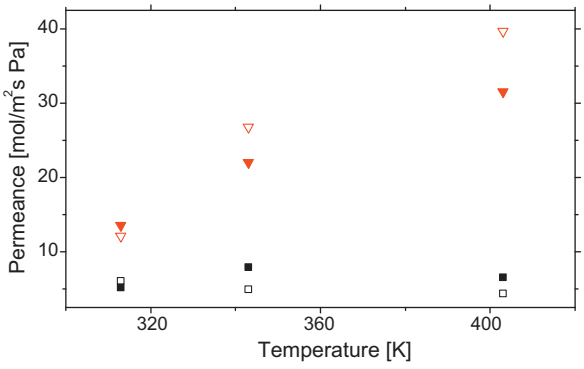

Fig. 12. Permeance as a function of the temperature for benzene (■)/p-xylene (▼) (578.7 Pa/322.9 Pa) mixtures (filled symbols) compared to the single components (unfilled symbols) with Silicalite-1 in Wicke–Kallenbach experiments at 343, 373 and 403 K.

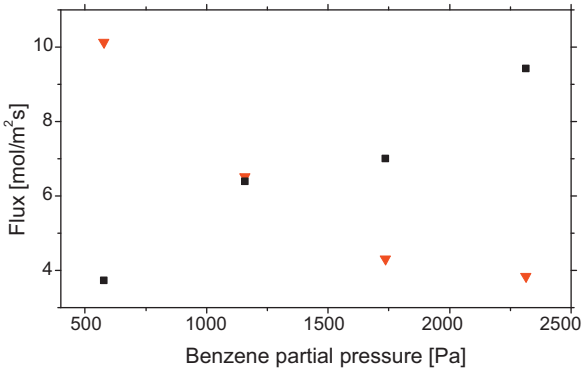

Fig. 13. Permeation flux of benzene (■) and p-xylene (▼) at varying benzene partial pressures using Silicalite-1 membrane in a Wicke–Kallenbach experiment at 403 K. The p-xylene concentration was kept constant at 322.9 Pa.

In order to determine the influence of the partial pressure of benzene and p-xylene on the permeation flux, the partial pressure of benzene in the feed was varied between 579 and 2315 Pa, while the p-xylene concentration was kept constant (Fig. 13). The result showed a linear increase of the benzene flux, whereas an exponential decay of the p-xylene permeation was observed.

4. Discussion

By comparing the transport characteristics in a single particle [13,20–22], in pellets and grown membranes (results presented in this publication) distinct differences become apparent. Previous studies showed that in isolated particles the diffusion of benzene is faster than that of p-xylene [13] and that the diffusion coefficients for p-xylene are non-isotropic due to the reorientations required when diffusing through the straight and the sinusoidal channel systems of MFI. In contrast, the diffusion of benzene is isotropic because of the possibility to easily re-orientate in the intersections in between the two channels. As mentioned before the diffusion coefficients in the small particles ($\sim 10^{-15}$ m^2/s) are about two orders of magnitude smaller than those obtained for larger particles [13,20–23]. For these (small) particles we have already shown by a detailed analysis of the transport network, that the overall process is determined by the surface adsorption (i.e., the sticking probability) and the pore entrance step and not by intracrystalline diffusion, as it is the case for larger particles ($\sim$3 μm) [13]. In contrast to previously reported steady state diffusivities [24] the data presented in this paper for the isolated ZSM-5 particles are transport diffusivities. Note, that this results in a difference of four orders of magnitude as the steady diffusivities are corrected by the loading of the zeolite. Nevertheless, the diffusion coefficients of p-xylene presented here are in line with the steady state diffusion coefficients from Garcia and Weisz [24].

To ensure that the transport diffusivities are not influenced by capillary condensation of the sorbent the limits for the partial pressures for benzene (2700 Pa) and p-xylene (700 Pa) at 313 K were calculated according to the macroscopic Kelvin equation [25]. These values are increasing markedly with the temperature indicating that capillary condensation plays a role neither in the frequency response nor in the Wicke–Kallenbach experiments.

The transport characteristic of a pellet with a thickness of 1 mm was significantly different to the isolated particles. The gravimetric uptake experiments clearly point to a shift in the rate determining step from processes on the surface (pore entrance) towards the diffusion inside the mesopores. This is supported by the fact that the time constants of diffusion measured by uptake experiments are two orders of magnitude larger than the time constants obtained in frequency response experiments on isolated particles [13]. The resulting diffusion coefficients of benzene and p-xylene in a pellet are 1.36×10^{-10} m^2/s and 4.33×10^{-12} m^2/s, respectively, which are three to five orders of magnitude larger compared to 7.34×10^{-15} m^2/s and 2.48×10^{-15} m^2/s observed for the isolated particles.

According to the Knudsen theory (Eq. (7)), the diffusion coefficients of the transport of benzene and p-xylene inside the mesopores are 6.36×10^{-7} and 5.45×10^{-7} m^2/s, respectively, assuming that the diameter of the smallest mesopores in the pellet (6 nm) controls the diffusion.

$$D_{K,eff} = \frac{\varepsilon_p}{\tau_F} * \frac{d_p}{3} * \sqrt{\frac{8RT}{\pi M}} \tag{7}$$

The comparison of the diffusion coefficients for diffusion in the micropores of isolated particles (10^{-15} m^2/s) [13] and in the mesopores (10^{-7} m^2/s) with that obtained in the adsorption experiments (10^{-10} m^2/s) indicates that the rate of adsorption in a pressed pellet is controlled by both processes.

Considering the results of the experiments in the Wicke–Kallenbach cell a few experimental details have to be discussed in detail first. These are (i) the time for the concentration front to pass through the pellet, (ii) the "overshooting" effect of the benzene concentration above the steady state concentration after the breakthrough and (iii) the molar fluxes under steady state conditions. All these effects can be explained by describing the pellet as a bed adsorber.

Note that the theoretical comparison of the uptake kinetics observed for benzene into particles to the transport inside the mesopores (controlled by Knudsen diffusion) supports the assumption of an adsorber. In order to calculate the transient diffusional flux and the adsorption kinetics, two models based on the Fickian law were used [17,26]. According to Ruthven et al. the uptake into an isolated particle in the case of micropore diffusion control can be described under isothermal conditions by Eq. (8) [26]:

$$\bar{Q}(t) = \frac{c_A - c_0}{c_A - c_\infty} = 1 - \frac{6}{\pi^2} \sum_{n=1}^{\infty} \left(\frac{1}{n^2} \exp\left(\frac{-n^2 \pi^2 D}{L^2} \right) \right) \tag{8}$$

In contrast, the solution of the Fickian law describing the diffusion through a membrane at initial conditions is given in Eq. (9) [17].

$$F(t) = -\left(\frac{D\delta c}{\delta x} \right)_{x=L} = 2c_F \sum_{n=1}^{\infty} \left(\frac{D}{\pi t} \right)^{\frac{1}{2}} \exp\left\{ \frac{-(2n+1)^2 L^2}{(4Dt)} \right\} \tag{9}$$

The simulated benzene uptake into a particle and the diffusional flux through a membrane are compared in Fig. 14. If the particles are surrounded by mesopores, it can be assumed that the characteristic length of diffusion L is equal to the particle size. The diffusion coefficient D was determined previously by frequency response experiments [13] and the diffusional length in the mesopores is equal to the thickness of the pellet (1 mm for the standard pellet). The diffusion coefficient based on the Knudsen theory can be calculates using the pore size obtained by DFT analysis of the N_2 sorption isotherm. The results of the simulation are presented in Fig. 14.

The time constant of the uptake into the bulk of the pellet was found to be much smaller than the transport through the mesopores, which is in line with the changes in the adsorption kinetics observed on the isolated particles and the pressed pellets. As the difference between the two processes is about one order of magnitude both processes influence the uptake kinetics. Furthermore, the simulation confirms the assumption that the pellet acts similar to a bed adsorber, as it shows that a molecule is faster adsorbed into the micropores of the particles surrounding the mesopores than diffusing through the mesopores in the pellet.

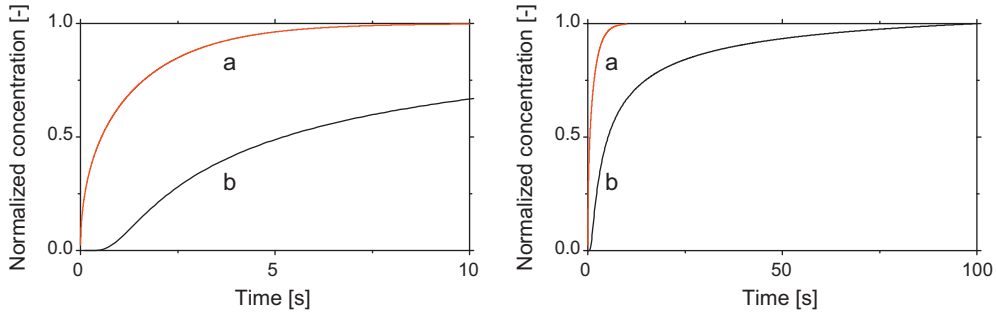

Fig. 14. Simulated plots of the normalized gravimetric (a) and the normalized initial flux (b) through a mesoporous membrane.

In this context it has to be noted that the time required to diffuse through the pellet depends on the sorption capacity of the material. The zeolite sample has a higher sorption capacity for p-xylene compared to benzene (i.e., about 1.5–1.7) [27], which leads to a longer breakthrough time of p-xylene. The time required for the concentration front to pass through the pellet was estimated by assuming that the flux into the pellet at the beginning of the experiment is identical with the steady state flux (described by Eq. (10)). The time needed by the concentration front to pass through the pellet was calculated according to Eq. (10). The theoretical and experimental values are compared in Table 8.

$$t_{transm.} = \frac{N_{UC} * SO_{\max}}{F * A} \quad (10)$$

The divergence between the experimentally and theoretically obtained data is about 20%. The theoretically calculated values are generally higher (except for one) than the experimental data, which is attributed to the competitive adsorption decreasing the maximum loading of benzene and p-xylene. The direct relation of the time required for the concentration front to pass through the pellet and the sorption capacity shows that the transport process is controlled by the sorption capacity (thermodynamics) rather than the transport rates in the mesopores (kinetic effect).

The adsorption enthalpies of 94 kJ/mol and 51 kJ/mol for p-xylene and benzene, respectively, can be used to explain the "overshooting" effect observed for benzene (Figs. 7 and 9) according to the theory of an adsorber bed. The weaker adsorbing substance (i.e. benzene) passes first through the bed and shows a characteristic "overshooting", because it is replaced from the sorption sites by the stronger interacting, but slower diffusing second component (i.e. p-xylene), which shows an exponential time dependence for the transport through the pellet. Once the adsorption–desorption equilibrium is established, the concentrations of benzene and p-xylene passing through the pellet are independent of the time.

The most significant results of the Wicke–Kallenbach experiments are the flux and permeance ratios at steady state conditions. For the pressed pellets the permeabilities of benzene and p-xylene are equal and their ratio is independent of the temperature and pellet thickness. The separation factor of one shows that a separation of these two aromatic components is not possible with a pressed pellet. Furthermore, the permeances are two orders of magnitude higher than in crystalline membranes. The diffusion coefficients for the benzene and p-xylene measured in the Wicke–Kallenbach cell were between 3.6 and 7.2×10^{-7} m^2/s, which can be related to an average pore diameter of 6.3 nm assuming Knudsen diffusion. This is consistent with the DFT analysis of the nitrogen sorption isotherm (Fig. 2) and indicates that the steady state fluxes are controlled by the transport through interparticle mesopores. This allows describing the transport through the pressed pellet by two contributions. (i) The transient behavior, which results from the adsorption equilibrium and not from the intra- and interparticle diffusion. (ii) The steady state conditions, where the transport is solely controlled by Knudsen diffusion in the interparticle mesopores and consequently, the smallest pores determine the overall flux. Therefore, the separation inside the pellet is a process controlled by sorption equilibria (thermodynamics), while the permeability is determined by mesopore diffusion (kinetic effect).

Although the actual results confirm that it is impossible to separate aromatic molecules with pressed pellets of ZSM-5, it has a significant impact on the understanding of transport processes in extrudates because the ZSM-5 pellets can be seen as model systems for larger particles made by extrusion. The time constants of diffusion increased by two orders of magnitude from isolated particles to the compacted pellets of 1 mm thickness for benzene and p-xylene. This indicates the existence of an intra-particle diffusion limitation in the pressed particles, which allows establishing the sorption equilibrium over the individual particles. To avoid the limitation by intra particle diffusion the pore sizes in extrudates have to be enlarged. Rodrigues et al. indicated that effectiveness of chromatographic processes can be increased by using materials with larger pores as the effective diffusivity is augmented by convection [28]. Note that the selectivity of reactions will be influenced by re-adsorption. Certainly, reactions depending on the uptake characteristics of individual particles such as the shape selective toluene alkylation will face decreasing selectivity due to the enhanced adsorption rate of the product molecules during the retarded diffusion processes in the mesopores.

An entirely different transient and steady state transport regime was observed in crystalline Silicalite-1 membranes. Benzene showed a similar "overshooting" effect under transient conditions at 313 K as in the pressed pellets, but this effect disappeared at 403 K. This indicates that the transport is controlled by a combination of adsorption and micropore diffusion, which can be described assuming a generalized Stefan–Maxwell diffusion for-

Table 8
Comparison of the experimentally and theoretically obtained breakthrough times of benzene and p-xylene through a of ZSM-5 pellet at 343, 373 and 403 K as well as different weights of 50, 100 and 150 mg.

T [K]	Pellet-weight [mg]	$t_{Ex.,benzene}$ [min]	$t_{Ex.,p\text{-}xylene}$ [min]	$t_{theo.,benzene}$ [min]	$t_{theo.,p\text{-}xylene}$ [min]
343	100	19	47	23	54
373	100	12	27	15	29
403	100	7	17	7	15
373	50	3	9	5	13
373	150	23	47	33	71

malism [29,32]. At low temperatures the adsorption is decisive for the transient concentration curve because the surface coverages are generally high. Therefore, in binary mixtures the competitive adsorption leads to an "overshooting" of the concentration of the weaker adsorbing substance in the transient concentration profile [32]. As the surface coverage decreases with increasing temperature (by 75% from 313 K to 403 K) [27] and the diffusion coefficient increases at the same time, the impact of the competitive adsorption on the concentration profile decreases with increasing temperature (Fig. 11).

To allow the prediction of the fluxes across membranes in binary systems by the Stefan–Maxwell theory the (Stefan–Maxwell) diffusion coefficient, the density of the material, the surface coverage as well as its gradient through the pellet [29,30] are required. According to the Stefan–Maxwell theory the transport of a binary mixture through a membrane can be described by Eq. (11) [31]:

$$F_1 = -q_{sat}\rho\frac{D_1^{SM}}{(1-\theta_1-\theta_2)}[(1-\theta_2)\nabla\theta_1 + \theta_1\nabla\theta_2] \quad (11)$$

This equation is valid for the special case of (binary) diffusion without interactions between the diffusing molecules. As the partial pressures of benzene and p-xylene were low, this boundary condition can be assumed as fulfilled and the equation can be used for describing the diffusion in the membrane.

In contrast to Fickian formalism, Stefan–Maxwell diffusion describes a situation, where the surface occupation plays a decisive role for the transport. According to Bakker et al. [32], the adsorption strength is decisive for the separation selectivity. Due to competitive adsorption the surface occupancy of the weaker adsorbing substance is lowered, which in turn enhances the transport selectivity towards the stronger adsorbing substance. Although the saturation limit of benzene and p-xylene on ZSM-5 is 8 molecules per unit cell [27], the relative surface coverage of p-xylene is about 1.5 times higher in the pressure range of 10^2 to 5×10^3 Pa. As a consequence the p-xylene permeance exceeds that of benzene by a factor of 2.6–5 in accordance to the Stefan–Maxwell theory, which relates the faster transport of p-xylene compared to benzene to the higher relative surface coverage at elevated temperatures [27].

This can be confirmed by the observation that the flux of benzene increases with increasing partial pressure in the feed, while at the same time the p-xylene flux decreased (Fig. 13). This experiment indicates that the permeation flux in this system can be directly related to the surface coverage and the description in terms of the Stefan Maxwell formalism is valid (In contrast Fickian diffusion would predict that the permeation flux is independent of the surface coverage). Opposite trends for benzene and p-xylene were observed when comparing the membrane permeances of the single components to that of the mixtures (Fig. 11). An increase of the permeability with increasing temperature was observed for benzene in comparison to the single component, whereas the permeability decreased for p-xylene. Krishna and van Baten showed in previous theoretical studies on C1 to C3 mixtures that the transport of the more mobile species in a mixture is slowed down, whereas the transport of the slower component is enhanced at the same time for zeolites with intersecting channel systems such as MFI, ISV and BEA [33,34].

Another important result is that the single gas permeation of benzene is decreasing with increasing temperature, whereas it is increasing for p-xylene. This finding is interesting, because an opposite trend is observed with isolated ZSM-5 particles for benzene. The permeance of a membrane depends on the diffusivity and the surface coverage (Eq. (12)). As the diffusivity increases with the temperature, while the surface coverage decreases, the latter must be responsible for the temperature dependency observed [35].

$$F_1 = -q_{sat}\rho\frac{D_1^{SM}}{(1-\theta_1)}\nabla\theta_1 \quad (12)$$

Referring to previous publications, a maximum of the flux is found when the activation energy of diffusion is smaller than heat of adsorption [30]. Eq. (13) was developed from generalized Stefan–Maxwell equations and it indicates that the maximum of the flux is obtained when the logarithmic mean of the free vacancies equals to the ratio of activation energy of diffusion and heat of adsorption [30].

$$(1-\theta_i)_{\ln} = \frac{E_{A,D}}{\Delta H_{Ads}} \quad (13)$$

Hence, the maximum of the permeability depends on the coverage, the thickness of the membrane as well as on the feed concentration of the diffusing substance. Consequently, the number of free vacancies increases with the membrane thickness because the molecular flux is decreasing and thus, the maximum of the flux is reached at lower temperatures. It has been also observed that the maximum permeability temperature decreases with decreasing feed concentration due to lower surface coverage at decreased feed concentrations [30]. In the system examined, the maximum permeance of benzene is below 313 K whereas the maximum of p-xylene seems to be above 403 K. This is once more an effect of the higher surface coverage of p-xylene in comparison to benzene [30].

5. Conclusions

The transport characteristics of benzene and p-xylene in MFI change significantly between single particles, pressed pellets and grown membranes. In isolated particles, diffusion can be described by the Fickian law resulting in a faster diffusion of benzene compared to p-xylene. A different transport mechanism occurs in pressed pellets, where the uptake into the bulk is controlled by a combination of micro- and mesoporous diffusion. The transient transport behavior of benzene and p-xylene in a pellet depends on its adsorption capacity, while the steady state permeability is solely controlled by Knudsen diffusion in the mesopores leading to identical permeances for benzene and p-xylene (independent of the temperature or the pellet thickness). Under these conditions the pressed pellets behave like a (classical) bed adsorber and do not allow a separation of these molecules.

On the Silicalite-1 membrane, the permeabilities are in general two orders of magnitude lower compared to the pressed pellet. In contrast to the pressed pellets, the transport under transient and steady state conditions can be described by the Stefan–Maxwell model. The transient behavior of mixtures of benzene and p-xylene showed a strong temperature dependency and is controlled by a combination of adsorption and micropore diffusion. The enhanced permeability of p-xylene compared to benzene at steady state conditions allows an enrichment of p-xylene in the effluent stream.

This work shows that in transport processes a pellet can be understood as an analogue of an extrudate. Consequently, the transport processes observed can be readily extended to the application of hierarchical materials for diffusion controlled separations and reactions. The steady state flux is only controlled by the diffusion in the mesopores, while the sorption equilibrium over the individual particles is established. Therefore, the sorption properties of the particles do not influence the overall transport characteristics in the pellet. The transport through the micropores of a membrane, in contrast, is controlled by configurational diffusion at low partial pressure (or coverage), which allows the separation of the aromatic molecules. Unfortunately, the transport in the mixture changes to single file diffusion at high loadings,

where the permeability is controlled by the flux of the slower diffusing molecules. Therefore, the separation in the industrial relevant pressure range is limited, which narrows the applicability of membrane separation techniques.

Acknowledgements

The authors acknowledge the support from Ministry of Higher Education, Saudi Arabia for the establishment of the Center of Research Excellence in Petroleum Refining and Petrochemicals at King Fahd University of Petroleum and Minerals (KFUPM).

The financial support from the Deutsche Forschungsgemeinschaft DFG under project JE260-8/1 is acknowledged. Robin Kolvenbach acknowledges the "Fonds der chemischen Industrie" for financial support by a Ph.D. scholarship. The authors are also grateful to Martin Neukamm for conducting the SEM measurements, and for the fruitful discussions in the framework of the center of excellence IDECAT.

References

[1] T.Y. Yan, Ind. Eng. Chem. Res. 28 (1989) 572.
[2] G. Xomeritakis, M Tsapatsis, Chem. Mater. 11 (1999) 875.
[3] G. Xomeritakis, S. Nair, M. Tsapatsis, Micropor. Mesopor. Mater. 38 (2000) 61.
[4] G. Xomeritakis, Z. Lai, M. Tsapatsis, Ind. Eng. Chem. Res. 40 (2001) 544.
[5] J. Perez-Ramirez, C.H. Christensen, K. Egeblad, C.H. Christensen, J.C. Groen, J. Chem. Soc. Rev. 37 (2008) 2530.
[6] K. Keizer, A.J. Burggraaf, Z.A.E.P. Vroon, H. Verweij, J. Membr. Sci. 147 (1998) 159.
[7] H. Sakai, T. Tomita, T. Takahashi, Sep. Purif. Technol. 25 (2001) 297.
[8] M.O. Daramola, A.J. Burger, M. Pera-Titus, A. Giroir-Fendler, S. Miachon, L. Lorenzen, J. Membr. Sci. 337 (2009) 106.
[9] Z. Deng, C.-H. Nicolas, M.O. Daramola, J. Sublet, Th. Schiestel, A.J. Burger, Y. Guo, A. Giroir-Fendler, M. Pera-Titus, J. Membr. Sci. 1 (2010) 364.
[10] C.D. Baertsch, H.H. Funke, J.L. Falconer, R.D. Noble, J. Phys. Chem. 100 (1996) 7676.
[11] C.J. Gump, V.A. Tuan, R.D. Noble, J.L. Falconer, Ind. Eng. Chem. Res. 40 (2001) 565.
[12] J.B. Lee, H.H. Funke, R.D. Noble, J.L. Falconer, J. Membr. Sci. 341 (2009) 238.
[13] O.C. Gobin, S.J. Reitmeier, A. Jentys, J.A. Lercher, J. Phys. Chem. C 113 (2009) 20435.
[14] S. Zheng, H.R. Heydenrych, A. Jentys, J.A. Lercher, J. Phys. Chem. B 106 (2002) 9552.
[15] Y. Yasuda, Heterogen. Chem. Rev. 1 (1994) 103.
[16] N. Hansen, The CMA evolution strategy: a comparing review, in: J.A. Lozano, P. Larranaga, I. Inza, E. Bengoetxea (Eds.), Towards a New Evolutionary Computation. Advances on Estimation of Distribution Algorithms, Springer, New York, 2006, p. 75.
[17] J. Crank, The Mathematics of Diffusion, Oxford University Press, 1979.
[18] S. Brunauer, P.H. Emmett, E. Teller, J. Am. Chem. Soc. 60 (1938) 309.
[19] M.J. Kruk, J. Choma, Carbon 36 (1998) 1447.
[20] S.J. Reitmeier, O.C. Gobin, A. Jentys, J.A Lercher, Angew. Chem. Int. Ed. 48 (2009) 533.
[21] O.C. Gobin, S.J. Reitmeier, A. Jentys, J.A. Lercher, Micropor. Mesopor. Mater. 125 (2009) 3.
[22] S.J. Reitmeier, O.C. Gobin, A. Jentys, J.A. Lercher, J. Phys. Chem. C 113 (2009) 15355.
[23] L. Song, L.V.C. Rees, Micropor. Mesopor. Mater. 301 (2000) 35–36.
[24] S.F. Garcia, P.B. Weisz, J. Catal. 121 (1990) 294.
[25] P.B. Weisz, Ind. Eng. Chem. Res. 34 (1995) 2692.
[26] D.M. Ruthven, L.K. Lee, H. Yucel, AlChE J. 26 (1980) 16.
[27] R.R. Mukti, A. Jentys, J.A. Lercher, J. Phys. Chem. C 111 (2007) 3973.
[28] A.E. Rodrigues, J.C. Lopez, Z.P. Lu, J.M. Loureiro, M.M. Dias, J. Chromatogr. 93 (1992) 590.
[29] J.M. van de Graaf, F. Kapteijn, J.A. Moulijn, AlChE J. 45 (1999) 497.
[30] F. Kapteijn, J.M. van de Graaf, J.A. Moulijn, AlChE J. 46 (2000) 1096.
[31] R. Krishna, Gas Sep. Purif. 7 (1993) 91.
[32] W.J.W. Bakker, F. Kapteijn, J. Poppe, J.A. Moulijn, J. Membrane. Sci. 117 (1996) 57.
[33] R. Krishna, J.M. van Baten, Micropor. Mesopor. Mater. 107 (2008) 296.
[34] R. Krishna, J.M. van Baten, J. Phys. Chem. B 109 (2005) 6386.
[35] F. Kapteijn, W.J.W. Bakker, G. Zheng, J.A. Moulijn, Micropor. Mesopor. Mater. 3 (1994) 227.